AIAA JOURNAL
Vol. 33, No. 5, May 1995

# Interaction of Local and Global Nonlinearities of Elastic Rotating Structures

Udo Hänle,* Dieter Dinkler,† and Bernd Kröplin‡
*University of Stuttgart, 70569 Stuttgart, Germany*

**Geometrically nonlinear effects like buckling due to large acceleration of lightweight and thin walled structures often play an important role in flexible multibody dynamics. To account for the interaction between local and global nonlinearities, a generalized method to model the motion of large flexible elastic structures is applied. The structure is decomposed into substructures, which are discretized using the finite element method. To reduce the number of degrees of freedom, a set of well-suited modes for the description of the displacement field on substructure level is used. The formulation introduced here combines the advantages of the corotational finite element formulation and the component mode synthesis method, resulting in a reduced set of degrees of freedom including local nonlinearities on substructure level.**

## Introduction

INVESTIGATIONS into the dynamic behavior of large structures undergoing finite displacements are expensive due to the large amount of computing time required. To reduce the numerical effort, several methods based on substructuring and natural mode decomposition of the displacement field have been developed.[1,6,9,10,12] Current applications are primarily limited to linear oscillation behavior of general elastic structures. In most cases nonlinearities are incorporated only for beam-like structures having rigid cross sections. To consider both global (finite rotations) and local (for example, dynamic buckling) nonlinearities, the proposed procedure is based on the following steps:

1) Decomposition of the structure into elastic substructures and discretization of the substructures (for example, a robot manipulator) is accomplished using a finite element formulation applied to a shell theory of moderately large (linearized) rotations. To simplify the nonlinearity with respect to the deformation, the derivation of the Euler–Lagrange equations and their consistent linearization is performed by using a mixed Hellinger–Reissner formulation, where the nonlinearities are of second order.

2) Reduction of the number of degrees of freedom is achieved by means of component modes and the subsequent transformation of the inertia and nonlinear stiffness matrices into the reduced subspace on substructure level. The component modes for the condensation satisfy the continuity between adjacent substructures using unit displacement modes and describe the dynamic behavior within the substructures by hand of internal vibration modes. To account for the local buckling phenomena, additional static modes are used, which are adapted to the nonlinear deformation behavior.

3) The reduced substructure matrices are embedded in a corotational formulation for handling the finite rotations of the overall structure.

## Kinematics

### Configuration

In continuum mechanics, the term configuration refers to the deformed state of a body $B$, specified by the invertible mapping $\Phi: B \to \mathcal{R}^3$. Depending on the state of deformation, one may distinguish between the reference configuration $\Phi = \mathrm{id}$ (identity) and the deformed configuration. Points on $B$ are identified by coordinates $X^A$ $(A = 1, 2, 3)$, and points $\Phi(X)$ by coordinates $x^a$ $(a = 1, 2, 3)$. The time-dependent motion of $B$ is described by the one-parameter mapping (integral curve) $t \to \Phi_t$, $t \in \mathcal{R}$.

### Geometric Description

Because of the underlying Euclidean space, a displacement field $\boldsymbol{U}(X)$ may be introduced, which describes the displacements of material points on $B$. The position of these points may be given in components with respect to the arbitrary vector bases $\boldsymbol{E}_A$, $\boldsymbol{e}_a$ $(A, a = 1, 2, 3)$ according to Fig. 1:

$$Y^A = U^A + X^A = (Y_0)^A + (T_0)^A_a x^a \tag{1}$$

Using the orthogonal transformation $\boldsymbol{T}_0 \in SO(3)$, a transformation of the vector bases from $\boldsymbol{E}_A$ to $\boldsymbol{e}_a$ gives

$$y^a = u^a + \left(\boldsymbol{T}_0^T\right)^a_A X^A = (y_0)^a + x^a \tag{2}$$

where the index $(\cdot)_0$ refers to the position and orientation of the moving coordinate system $\{x^i\}$.

The kinematic descriptions of Eqs. (1) and (2) depend on an orthogonal mapping $\boldsymbol{T}$, which is an element of the nonlinear manifold $SO(3)$. In the Appendix, a short introduction to orthogonal transformations is given to establish the notation used and to show important kinematic relationships.

## Energy Functions

The kinematic description is based on the assumption that the resulting strains are small, although the rigid body displacements of the motion $\Phi_t$ are without restriction. In the presented application of a thin walled tube, for the reduction of the continuum to a shell reference surface the Kirchhoff–Love hypothesis[11] is used. In addition, the theory of moderate (linearized) rotations is applied, where the nonlinear terms for the description of the curvature of the reference surfaces are neglected.[8]

Since the assumption of small strains is to be used, the rigid body displacements can be kinematically separated from the deformation. For this purpose, a corotational formulation divides the displacement field into a deformation part with respect to a moving coordinate system and a rigid body part. This concept coincides with the kinematic equations (1) and (2), if the vector bases $\boldsymbol{e}_a$ are fixed to the body.

According to Fig. 1, the relative displacement $\boldsymbol{x}$ can be separated by using $\boldsymbol{x} = \boldsymbol{x}|_{W=0} + \boldsymbol{c}$, where $\boldsymbol{x}|_{W=0} = (\boldsymbol{x}|_{W=0})^i \boldsymbol{e}_i$ are the coordinates of a point in the undeformed state with respect to the moving coordinate system $\{x^i\}$. $W$ is the strain energy of a body. Applying the separation of the displacements, the deformation gradient

Received Feb. 19, 1994; presented as Paper 94-1674 at the AIAA Dynamic Specialist Conference, Hilton Head, SC, April 21–22, 1994; revision received Aug. 24, 1994; accepted for publication Aug. 24, 1994. 

*Research Assistant, Institute for Statics and Dynamics of Aerospace Structures. Member AIAA.

†Professor, Institute for Statics and Dynamics of Aerospace Structures.

‡Professor, Head of Institute for Statics and Dynamics of Aerospace Structures.

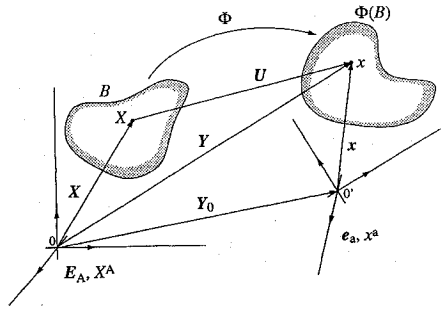


**Fig. 1 Geometric description of the continuum.**

$\boldsymbol{F} = F_B^a\, \boldsymbol{e}_a \otimes \boldsymbol{E}^B$ of the motion $\Phi_t$ yields

$$F_B^a = \left(\boldsymbol{T}_0^T\right)_B^a + \frac{\partial c^a}{\partial X^B} \tag{3}$$

**Strain Energy of the Body**

Assuming ideally elastic material (generalized Hookes law), the strain energy $W$ of a body is given by

$$W = \frac{1}{2}\int_V \boldsymbol{S}:\boldsymbol{E}\,\mathrm{d}V = \frac{1}{2}\int_V S^{AB}E_{AB}\,\mathrm{d}V \tag{4}$$

where $\boldsymbol{E}$ is the Green strain tensor

$$E_{AB} = \tfrac{1}{2}\left(F_A^a\, g_{ab}\, F_B^b - G_{AB}\right) \tag{5}$$

and $\boldsymbol{G}$ is the metric tensor of the reference configuration, $\boldsymbol{g}$ the metric tensor of the deformed configuration, $\boldsymbol{S}$ the second Piola–Kirchhoff stress tensor,[7] and $V$ the volume of the reference configuration. Summation convention, which means the summation on repeated indices, is used in the preceding equations. Substituting the stress tensor $\boldsymbol{S}$ by applying the material law leads to the pure strain formulation

$$W = \frac{1}{2}\int_V \boldsymbol{E}:\boldsymbol{C}:\boldsymbol{E}\,\mathrm{d}V \tag{6}$$

where $\boldsymbol{C}$ is the elasticity of the material, which is of fourth order with respect to the deformation, see Eqs. (3) and (5). In an alternative way, the strain energy may also be described using stresses and strains in a mixed Hellinger–Reissner formulation[11]

$$W = \int_V \left(\boldsymbol{S}:\boldsymbol{E} - \tfrac{1}{2}\boldsymbol{S}:\boldsymbol{\mathcal{D}}:\boldsymbol{S}\right)\mathrm{d}V \tag{7}$$

where $\boldsymbol{\mathcal{D}}$ is the flexibility of the material. As a result of Eq. (7), nonlinearities are reduced by order one, maintaining general validity.

**Kinetic Energy of the Body**

The kinetic energy of a moving elastic body is calculated according to Fig. 1 by integration over the reference volume $V$

$$T = \frac{1}{2}\int_V \rho_{\mathrm{ref}}\left(\dot{\boldsymbol{Y}}^T\dot{\boldsymbol{Y}}\right)\mathrm{d}V \tag{8}$$

Using the left-invariant angular velocity $\tilde{\Omega} \in T_1 SO(3)$ (see the Appendix), the time derivative of Eq. (1) yields

$$\dot{\boldsymbol{Y}} = \dot{\boldsymbol{Y}}_0 + \boldsymbol{T}_0\dot{\boldsymbol{x}} + \boldsymbol{T}_0\tilde{\boldsymbol{\Omega}}_0\boldsymbol{x} \tag{9}$$

## Discretization

Using isoparametric finite elements, the interpolation of the relative position vector $\boldsymbol{x}$ to a point $x \in \Phi(B)$ of element $J$ is described by[9]

$$\boldsymbol{x}^{(J)} = \boldsymbol{T}^{(J)}\boldsymbol{N}^{(J)}\bar{\boldsymbol{T}}^{(J)}\boldsymbol{B}_1^{(J)}\left(\underline{\boldsymbol{x}}|_{W=0} + \boldsymbol{B}_2\underline{\boldsymbol{c}}\right) \tag{10}$$

$$\boldsymbol{X}^{(J)} = \bar{\boldsymbol{N}}^{(J)}\left(\underline{\boldsymbol{x}}|_{W=0} + \boldsymbol{B}_2\underline{\boldsymbol{c}}\right) \tag{11}$$

where the symbols are defined as follows.

$\boldsymbol{B}_1^{(J)}$ = Boolean matrix mapping element DOF into substructure DOF
$\boldsymbol{B}_2$ = Boolean matrix to eliminate the rigid body modes
$\underline{\boldsymbol{c}}$ = nodal degrees of freedom
$\boldsymbol{N}^{(J)}$ = complete matrix of shape functions
$\boldsymbol{T}^{(J)}$ = orthogonal transformation between the element coordinate system and $\{x^i\}$
$\bar{\boldsymbol{T}}^{(J)}$ = orthogonal transformation between nodal DOF of the substructure and the element $J$
$\underline{\boldsymbol{x}}|_{W=0}$ = discrete geometric description in the undeformed state

**Strain Energy**

To use the advantage of the mixed Hellinger–Reissner approach for the discrete weak form, the derivation of the internal reactions will be based on Eq. (7). Substituting the Green strain tensor by the deformation gradient $\boldsymbol{F}$, discretization and integration of the strain energy formulation over the reference volume $V$ leads to

$$W = \tfrac{1}{2}\underline{\boldsymbol{z}}^T\boldsymbol{A}_{\mathrm{lin}}\underline{\boldsymbol{z}} + \tfrac{1}{6}\underline{\boldsymbol{z}}^T\boldsymbol{A}_1(\underline{\boldsymbol{z}})\underline{\boldsymbol{z}} \tag{12}$$

$$\boldsymbol{A}_{\mathrm{lin}} = \mathrm{const}$$

$$\boldsymbol{A}_1(\underline{\boldsymbol{z}}) = \mathcal{O}(\underline{z}^i)$$

where the first variation of $W$ yields the secant matrix[11]

$$\boldsymbol{A}_{\mathrm{sec}} = \boldsymbol{A}_{\mathrm{lin}} + \tfrac{1}{2}\boldsymbol{A}_1(\underline{\boldsymbol{z}}) \tag{13}$$

Note that $\boldsymbol{A}_{\mathrm{sec}}$ depends only by first order on the force/momentum and displacement/rotation quantities which are combined in vector $\underline{\boldsymbol{z}}$ of unknown nodal degrees of freedom. Linearization of Eq. (13) with respect to a fundamental state $\underline{\boldsymbol{z}}$ leads to

$$D[\boldsymbol{A}_{\mathrm{sec}}(\underline{\boldsymbol{z}})\underline{\boldsymbol{z}}]\cdot\Delta\underline{\boldsymbol{z}} = \boldsymbol{A}_{\mathrm{tan}}(\underline{\boldsymbol{z}})\Delta\underline{\boldsymbol{z}} \tag{14}$$

with the tangent matrix

$$\boldsymbol{A}_{\mathrm{tan}} = \boldsymbol{A}_{\mathrm{lin}} + \boldsymbol{A}_1(\underline{\boldsymbol{z}}) \tag{15}$$

**Kinetic Energy**

Discretizing the kinetic energy expression (8), the discrete form of Eq. (9) gives[9]

$$\dot{\boldsymbol{Y}}^{(J)} = \dot{\boldsymbol{Y}}_0 + \boldsymbol{T}_0\bar{\boldsymbol{N}}^{(J)}\boldsymbol{B}_2\dot{\underline{\boldsymbol{c}}} + \boldsymbol{T}_0\tilde{\boldsymbol{\Omega}}_0\bar{\boldsymbol{N}}^{(J)}\left(\underline{\boldsymbol{x}}|_{W=0} + \boldsymbol{B}_2\underline{\boldsymbol{c}}\right) \tag{16}$$

which results in the classical mass matrix of flexible multibody formulations.[9,12] In this paper, a different approach is applied,[6] where the rigid body motion and the (deformation) velocity are not separated in the nodal unknowns. This difference to other multibody formulations allows a complete separation between substructuring and the large rotation analysis. Using corotated total translational and angular velocities $\dot{\underline{\boldsymbol{y}}}$ as nodal degrees of freedom

$$\dot{\boldsymbol{y}}^{(J)} = \boldsymbol{T}_0^T\dot{\boldsymbol{Y}}^{(J)}$$

$$= \dot{\boldsymbol{y}}_0 + \bar{\boldsymbol{N}}^{(J)}\boldsymbol{B}_2\dot{\underline{\boldsymbol{c}}} + \tilde{\boldsymbol{\Omega}}_0\bar{\boldsymbol{N}}^{(J)}\left(\underline{\boldsymbol{x}}|_{W=0} + \boldsymbol{B}_2\underline{\boldsymbol{c}}\right) \tag{17}$$

$$\dot{\boldsymbol{y}}^{(J)} \to \bar{\boldsymbol{N}}^{(J)}\dot{\underline{\boldsymbol{y}}} \tag{18}$$

the discrete form of the kinetic energy is given by

$$T = \tfrac{1}{2}\dot{\underline{\boldsymbol{y}}}^T\boldsymbol{M}\dot{\underline{\boldsymbol{y}}} \tag{19}$$

The discretization of the corotated total velocity in Eq. (18) is not consistent to the discretization of the relative displacement vector $\boldsymbol{c}$ in the strain energy expression. This inconsistency vanishes for $\boldsymbol{c} \to \boldsymbol{0}$, which justifies the use of Eq. (18) instead of Eq. (17) on the condition that only small deformations occur.

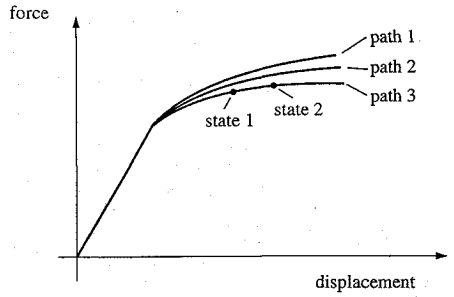


**Fig. 2 Possible states for static equilibrium modes.**

**Global Approximation**

The calculation of the dynamic behavior of complex structures using finite elements is not feasible in many cases without assuming some approximations leading to a reduction of degrees of freedom. This is particularly valid for the simulation of structures with geometric nonlinear deformation behavior in a time domain. If the decomposition of a structure into substructures is encouraged by the geometry, the deformation behavior of each substructure can be described by only a few component modes $\Psi = [\psi_1\ \psi_2\ \cdots\ \psi_n]$ without crucially limiting the accuracy. The displacement field approximated by $\underline{z}$ in Eq. (12) is substituted according to a modified form of the Craig–Bampton[3] modal synthesis method by the natural modes of the general eigenvalue problem of the unloaded substructure, the static equilibrium modes of the nonlinear problem to account for local nonlinear effects, and the unit displacement/rotation modes to satisfy the continuity between adjacent substructures.

In the following we will denote the first two kinds of modes as internal modes and the third as constraint modes.

To describe local geometrically nonlinear effects, the general rule is to enable the structure to deform along the lowest possible strain energy path. Therefore, at least, the states that describe the deformation along the lowest strain energy path must be used as transformation modes (see Fig. 2).

Applying the transformation

$$\underline{z} = \Psi \boldsymbol{q} \tag{20}$$

to Eq. (12) gives

$$W = \boldsymbol{q}^T \left[ \frac{1}{2} \bar{\boldsymbol{A}}_{\text{lin}} + \frac{1}{6} \sum_{l=1}^{n} \bar{\boldsymbol{A}}_l(\boldsymbol{q}) \right] \boldsymbol{q} \tag{21}$$

Vector $\boldsymbol{q}$ contains generalized coordinates $\eta_i$ for the internal modes and translational/rotational degrees of freedom with respect to the moving coordinate system

$$\boldsymbol{q}^T = \left[ (\boldsymbol{c}_1)^T \cdots (\boldsymbol{c}_k)^T \quad (\boldsymbol{\Theta}_{\text{rel}})_1^T \cdots (\boldsymbol{\Theta}_{\text{rel}})_l^T \quad \eta_1 \cdots \eta_m \right]$$

where $\boldsymbol{c}_1 \cdots \boldsymbol{c}_k$ are the displacement vectors for $k$ translational constraint mode triplets, $(\boldsymbol{\Theta}_{\text{rel}})_1 \cdots (\boldsymbol{\Theta}_{\text{rel}})_l$ are the rotation vectors for $l$ rotational constraint mode triplets, and $\eta_1 \cdots \eta_m$ are the participation factors for $m$ internal modes. Because of the fact that the strain energy expression is based on the mixed approach, the computational effort to calculate the strain energy is proportional only to the third power of $n$, where $n$ is the total number of transformation modes.

The transformation of the total velocity vector $\underline{\dot{y}}$ to the reduced space of generalized coordinates gives

$$\underline{\dot{y}} = \Psi_{\underline{\dot{y}}} \boldsymbol{D}^T \dot{\boldsymbol{r}} \tag{22}$$

which results in the reduced form of the kinetic energy expression

$$T = \tfrac{1}{2} \dot{\boldsymbol{r}}^T \boldsymbol{D} \bar{\boldsymbol{M}} \boldsymbol{D}^T \dot{\boldsymbol{r}} \tag{23}$$

where $\boldsymbol{D}$ is a hyperdiagonal matrix which transforms the translational velocities to the inertial frame. Vector $\dot{\boldsymbol{r}}$ contains total translational velocities, left invariant angular velocities, and the time derivative of the participation factors for the internal modes

$$\dot{\boldsymbol{r}}^T = \left[ (\dot{\boldsymbol{Y}}_0)^T \ (\boldsymbol{\Omega}_0)^T \quad \dot{\boldsymbol{Y}}_1^T \cdots \dot{\boldsymbol{Y}}_k^T \quad \boldsymbol{\Omega}_1^T \cdots \boldsymbol{\Omega}_l^T \quad \dot{\eta}_1 \cdots \dot{\eta}_m \right]$$

## Lagrange Equations

Finally, the discrete weak form of the governing equations are given by the nonlinear Lagrange equations, which are derived from the Lagrangian $L = T - \Pi$ when neglecting nonconservative generalized forces by

$$\frac{\mathrm{d}}{\mathrm{d}t}\left(\frac{\partial L}{\partial \dot{\boldsymbol{r}}}\right) - \frac{\partial L}{\partial \boldsymbol{r}} = \boldsymbol{F}_{\text{int}} + \boldsymbol{F}_{\text{iner}} - \boldsymbol{F}_{\text{appl}} = \boldsymbol{0} \tag{24}$$

$\Pi$ is the potential energy, the vector $\boldsymbol{F}_{\text{int}}$ denotes the elastic reactions, $\boldsymbol{F}_{\text{iner}}$ the inertia forces, and $\boldsymbol{F}_{\text{appl}}$ the applied (external) forces. The relation between the (deformation) displacements $\boldsymbol{c}_i$ and the total displacements $\boldsymbol{Y}_0$ and $\boldsymbol{Y}_i$ are given by Eq. (1). The relations between relative and total rotation quantities are given due to linearized rotations on substructure level by $\exp(\tilde{\boldsymbol{\theta}}_i) = \exp(\tilde{\boldsymbol{\theta}}_0)[1 + (\tilde{\boldsymbol{\Theta}}_{\text{rel}})_i]$ (see the Appendix).

Deriving the second term on the left side of Eq. (24), it becomes apparent that [according to Eqs. (40) and (41)] the left invariant angular velocities in the kinetic energy expression depends on the coordinate vector $\boldsymbol{r}$. Because of the fact that the generalized coordinate vector $\boldsymbol{r}$ does not separate the rigid body motion and the elastic deformation, the Lagrange equations of a substructure can be handled in the same way as is usually done for large displacement/rotation finite element formulations.

## Example

The validity of the derived formulation is shown for the benchmark example of a rotating beam in a previous publication.[4] Here, we will focus on local geometrically nonlinear effects (for example, dynamic buckling) and their consideration in the reduced model. Thus, a thin walled tube with an applied angular acceleration $\ddot{\phi}$ and an additional mass according to Fig. 3 is considered.

The time-dependent prescribed angular acceleration is

$$\ddot{\phi} = \begin{cases} -5.71\,t & \text{for } 0 \le t < 0.5 \\ -5.71 + 5.71\,t & \text{for } 0.5 \le t < 1.5 \\ 11.42 - 5.71\,t & \text{for } 1.5 \le t < 2 \\ 0 & \text{for } t \ge 2 \end{cases} \tag{25}$$

Taking symmetry into account, the tube is discretized using 800 shell elements in the mixed formulation (8019 unknowns) (see Fig. 4). The reduction is performed for model 1 in a conventional way by six unit displacement/rotation modes which are applied at each end cross section and 14 natural modes. The natural modes are calculated for clamped end cross sections (supressed coupling degrees of

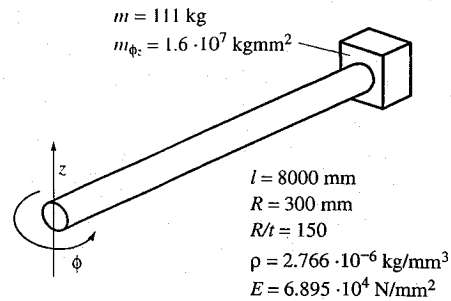


**Fig. 3 Accelerated thin-walled tube.**

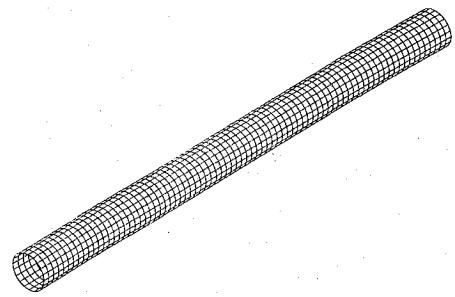

**Fig. 4 Finite element discretization.**

freedom[3]), so that the continuity to adjacent substructures is satisfied only by the constraint modes.

In a second reduction strategy (model 2), the last four natural modes are replaced by four static equilibrium modes. To calculate the static modes, a variable force $\pm P$ is applied at the end cross section of the tube according to Fig. 5.

The resulting load/deformation behavior $+P$ over $w$ is given for different equilibrium paths in Fig. 6. The equilibrium state $C$ and $D$ on the lowest path are chosen for $\pm P$ as reduction modes. Since these four modes have to be given for suppressed boundary conditions (internal modes), the corresponding weighted linear unit displacement modes must be subtracted from the static equilibrium modes to receive artificial clamped end conditions.

The comparison between the reduced model 1, the reduced model 2, and the full model is given in Fig. 7 for the characteristic load and the lowest calculated equilibrium path.

Note that the reduced model 1 is not able to reproduce the geometrically nonlinear static deformation behavior. It is important that model 1 is nearly identical to a model without internal modes and, therefore, to the beam discretization usually used.

In Fig. 8 the relative tip displacement after applying the prescribed angular acceleration [Eq. (25)] is shown for model 1 and model 2. The ovalization of the cross section and the local buckling result in a softening effect and, therefore, in a larger tip displacement. This becomes apparent when examining the participation factors $\eta_1$ and $\eta_2$ for the static equilibrium modes $\pm C$. Passing the bifurcation state $E$, the influence of these two modes change rapidly, indicating states of motion with high nonlinearity of the deformation behavior (Fig. 9).

Increasing the acceleration by $\dot{\Omega}_{new} = 1.5\,\dot{\Omega}_{old}$, the geometric nonlinearity leads to instability of the motion (see Figs. 10 and 11).

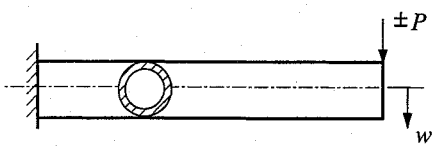


**Fig. 5 Local static deformation.**

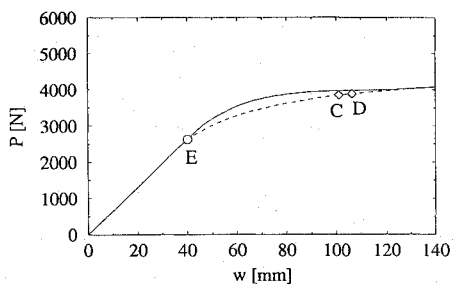


**Fig. 6 Equilibrium paths.**

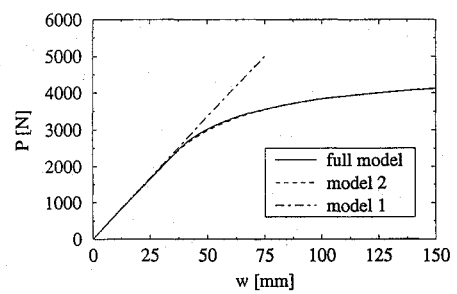


**Fig. 7 Accuracy of the reduced model.**

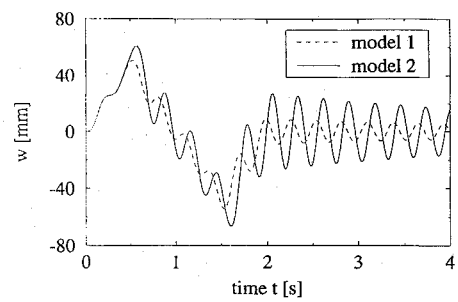


**Fig. 8 Tip displacement.**

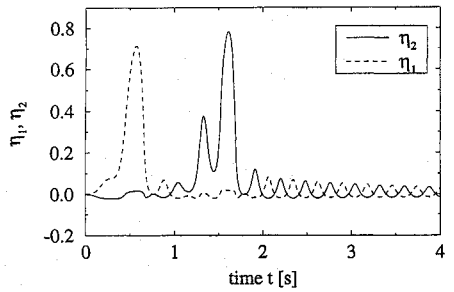


**Fig. 9 Participation factors for the modes $\pm C$.**

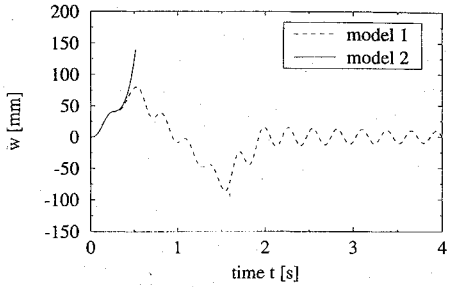


**Fig. 10 Instability of the motion.**

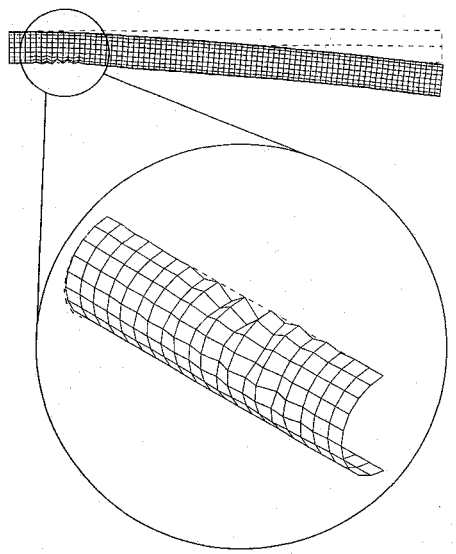

**Fig. 11 Local buckling.**

## Summary

Most of the multibody formulations presented in the literature are based on the finite element method for discretization of the continuum. In a second step, the subsequent reduction of the nodal unknowns is accomplished using global vibration modes.

In this context, the presented paper points out the advantages of using a reduced order of nonlinearity which as a result when taking a mixed Hellinger–Reissner formulation as a basis for the strain energy expression. If direct implicit time integration schemes together with a Newton–Raphson iteration are used, the application of static secant and tangent matrices and the exploitation of their similarity makes the computer implementation of the presented algorithm comparably easy.

Although geometrically nonlinear effects have been considered by many authors in flexible multibody systems, these global effects,

for example, geometric stiffening, only become apparent by a load-dependent coupling of the usually used reduction modes. However, local effects like dynamic buckling cannot be considered in the reduced subspace without calculating a new corresponding group of reduction modes and, therefore, a solution strategy for this kind of problem is demonstrated here.

## Appendix: Orthogonal Transformations

Succesive rotations are not commutative and the neccesity to distinguish between the order of two rotations leads to the following two mappings from the manifold $SO(3)$ onto itself.[2]

Left translation: $L_{T_1}: SO(3) \rightarrow SO(3)$

$$L_{T_1}(T_2) = T_1 \circ T_2 = T_1 T_2 \tag{A1}$$

Right translation: $R_{T_1}: SO(3) \rightarrow SO(3)$

$$R_{T_1}(T_2) = T_2 \circ T_1 = T_2 T_1 \tag{A2}$$

The induced linear mappings are defined by

$$L'_{T_1}(T_2): \qquad T_{T_2}SO(3) \rightarrow T_{T_1 T_2}SO(3) \tag{A3}$$

$$R'_{T_1}(T_2): \qquad T_{T_2}SO(3) \rightarrow T_{T_2 T_1}SO(3) \tag{A4}$$

Tangential vector fields $\tilde{a}(T)$ of the tangent space $T_T SO(3)$ are scewsymmetric for $T = \mathbf{1}$ (identity)

$$\tilde{a} = \tilde{a}(T)|_{T=1} = \tilde{a}^{ij} E_i \otimes E_j = -\varepsilon_k^{ij} a^k E_i \otimes E_j \tag{A5}$$

Vector fields that are of special importance in this context are ones which are invariant with respect to left or right translation.

Left invariant vector fields:

$$L'_{T_1}[\tilde{V}(T)] = \tilde{V}\big[L_{T_1}(T)\big] = \tilde{V}(T_1 T) = T_1 T \tilde{V} \tag{A6}$$

Right invariant vector fields:

$$R'_{T_1}[\tilde{v}(T)] = \tilde{v}\big[R_{T_1}(T)\big] = \tilde{v}(T T_1) = \tilde{v} T T_1 \tag{A7}$$

Although many large rotation finite element formulations are derived using right invariant (spatial) vector fields, the update process in direct implicit time integration schemes can be performed with less effort using the left invariant (material) vector fields.

Differentiating the orthogonal transformation with respect to the rotation angle $\phi$ leads to the first-order differential equation

$$\frac{dT}{d\phi} = T\tilde{n} = \tilde{n}T; \qquad \tilde{n} \in T_1 SO(3) \tag{A8}$$

where $n \in \mathcal{R}^3$ is the unit-length vector in the direction of the rotation axis (eigenvector of $T$ for the eigenvalue $\lambda = 1$). The homogeneous solution leads to the exponential mapping

$$\exp: T_1 SO(3) \rightarrow SO(3) \qquad \text{by} \qquad \tilde{\theta} \rightarrow \exp(\tilde{\theta}) \tag{A9}$$

with the rotation vector $\theta = \phi n$. Linearized transformations are given in tangent space $T_1 SO(3)$ by

$$\exp(\tilde{\theta}) \approx \mathbf{1} + \tilde{\theta} \tag{A10}$$

The Eulerian-like formulation of the variation of orthogonal transformations is given by

$$\frac{d}{d\varepsilon}[\exp(\varepsilon \Delta\tilde{\theta}) \exp(\tilde{\theta})]\Big|_{\varepsilon=0} = DT \cdot \Delta\tilde{\theta} = \Delta\tilde{\theta} \exp(\tilde{\theta}) \tag{A11}$$

$$\frac{d}{d\varepsilon}[\exp(\tilde{\theta}) \exp(\varepsilon \Delta\tilde{\Theta})]\Big|_{\varepsilon=0} = DT \cdot \Delta\tilde{\Theta} = \exp(\tilde{\theta}) \Delta\tilde{\Theta} \tag{A12}$$

Following Eqs. (A11) and (A12), the time derivative $\dot{T}$ in tangent space $T_T SO(3)$ may be written as

$$\frac{d}{dt} T(t) = \dot{T} = \tilde{\omega}(T, t) = \tilde{\omega}(\mathbf{1}, t) T(t) \tag{A13}$$

$$\frac{d}{dt} T(t) = \dot{T} = \tilde{\Omega}(T, t) = T(t) \tilde{\Omega}(\mathbf{1}, t) \tag{A14}$$

where $\tilde{\omega}(\mathbf{1}, t) = \tilde{\omega}(t)$ is the right invariant angular velocity and $\tilde{\Omega}(\mathbf{1}, t) = \tilde{\Omega}(t)$ is the left invariant angular velocity.

For a consistent linearization of the angular velocities $\tilde{\omega}$ and $\tilde{\Omega}$, it is important to recognize that the variations $\delta\tilde{\omega}$ and $\delta\tilde{\Omega}$

$$\delta\tilde{\omega} := \underbrace{\Delta\dot{\tilde{\theta}}}_{\text{part I}} + \underbrace{\frac{d}{dt}[\exp(t\,\Delta\tilde{\theta})\tilde{\omega}|_0 \exp(-t\,\Delta\tilde{\theta})]\Big|_{t=0}}_{\text{part II}}$$

$$= \Delta\dot{\tilde{\theta}} + \mathcal{L}_{\tilde{\omega}} \Delta\tilde{\theta}|_1 = \Delta\dot{\tilde{\theta}} + \Delta\tilde{\theta}\tilde{\omega} - \tilde{\omega}\Delta\tilde{\theta} \tag{A15}$$

$$\delta\tilde{\Omega} := \underbrace{\Delta\dot{\tilde{\Theta}}}_{\text{part I}} + \underbrace{\frac{d}{dt}[\exp(-t\,\Delta\tilde{\Theta})\tilde{\Omega}|_0 \exp(t\,\Delta\tilde{\Theta})]\Big|_{t=0}}_{\text{part II}}$$

$$= \Delta\dot{\tilde{\Theta}} - \mathcal{L}_{\tilde{\Omega}} \Delta\tilde{\Theta}|_1 = \Delta\dot{\tilde{\Theta}} - \Delta\tilde{\Theta}\tilde{\Omega} + \tilde{\Omega}\Delta\tilde{\Theta} \tag{A16}$$

not only depend on the change of $\dot{\tilde{\theta}}$ and $\dot{\tilde{\Theta}}$ for a fixed point on $SO(3)$ (part I), but also on the neighborhood of the point in question. Hence, part II of Eqs. (A15) and (A16) result from the parallel transport of $\omega$ or $\Omega$, which is equivalent to the Lie-derivative[2] $\mathcal{L}_{\tilde{\omega}} \Delta\tilde{\theta}|_1$ in case of right invariant vectors and $-\mathcal{L}_{\tilde{\Omega}} \Delta\tilde{\Theta}|_1$ in case of left invariant vectors.

## Acknowledgment

This work has been supported in part by the German Research Foundation (DFG) within the "Sonderforschungsbereich 349."

## References

[1]Banerjee, A. K., and Kane, T. R., "Dynamics of a Plate in Large Overall Motion," *Journal of Applied Mechanics*, Vol. 56, Dec. 1989, pp. 887–892.

[2]Choquet-Bruhat, Y., De Witt-Morette, C., and Dillard-Bleick, M., *Analysis, Manifolds and Physics, Part I: Basics*, North-Holland, London, 1982, pp. 152–168.

[3]Craig, R. R., and Bampton, M. C. C., "Coupling of Substructures for Dynamic Analysis," *AIAA Journal*, Vol. 6, July 1968, pp. 1313–1319.

[4]Dinkler, D., Hänle, U., and Kröplin, B., "Dynamics of Flexible Elastic Structures with Geometric Nonlinearities," *Dynamics and Control of Structures in Space*, Computational Mechanics, Southampton, Boston, MA, 1993, pp. 61–73.

[5]Dinkler, D., and Kröplin, B., "Dynamic Stability of Buckling Elastic Structures," *Dynamics of Flexible Structures in Space*, Computational Mechanics and Springer Verlag, London, 1990, pp. 449–460.

[6]Géradin, M., and Cardona, A., "The Co-Rotational Approach to Substructuring for Flexible Multibody Analysis," *Finite Elements in the 90's*, Springer Verlag/Centro Internacional de Métodos Numéricas en Ingeniería, Barcelona, Spain, 1991, pp. 285–295.

[7]Marsden, J. E., and Hughes, T. J. R., *Mathematical Foundation of Elasticity*, Prentice Hall, Englewood Cliffs, NJ, 1983.

[8]Schmidt, R., and Pietraszkiewicz, W., "Variational Principles in the Geometrically Non-Linear Theory of Shells Undergoing Moderate Rotations," *Ingenieur-Archiv*, Vol. 50, No. 3, 1981, pp. 187–201.

[9]Shabana, A. A., *Dynamics of Multibody Systems*, Wiley, New York, 1989.

[10]Wallrapp, O., Santos, J., and Ryu, J., "Superposition Method for Stress Stiffening in Flexible Multibody Dynamics," *Dynamics of Flexible Structures in Space*, Computational Mechanics and Springer Verlag, London, 1990, pp. 233–247.

[11]Washizu, K., *Variational Methods in Elasticity and Plasticity*, 2nd ed., Pergamon, New York, 1975.

[12]Yoo, W. S., and Haug, E. J., "Dynamics of Articulated Structures, Part I: Theory," *Journal of Structural Mechanics*, Vol. 14, No. 1, 1986, pp. 105–126.